# Eco-compatible protective treatments on an Italian historic mortar (XIV century)

G. Taglieri[a], V. Daniele[a*], G. Rosatelli[b], S. Sfarra[a], M.C. Mascolo[c], C. Mondelli[d]

[a] *Department of Industrial and Information Engineering and Economics, University of L'Aquila, Piazzale E. Pontieri 1, I-67100, Monteluco di Roio, Roio Poggio, L'Aquila (AQ), Italy; *valeria.daniele@univaq.it; Tel. 0039 862 434234; Fax 0039 862 434206*

[b] *Department of Psychological, Humanistic and Territorial Sciences, University of Chieti, Via dei Vestini 31, I-66100 Chieti (CH), Italy*

[c] *Department of Civil and Mechanical Engineering, University of Cassino and Southern Lazio, Via G. Di Biasio 43, I-03043 Cassino (FR), Italy*

[d] *CNR-IOM, Institut Laue Langevin, 71 Rue des Martyrs 38042 Grenoble Cedex 9, France*

**Abstract.** This paper reports significant results about the effects of repeated treatments to protect a mediaeval Italian mortar from capillarity-absorbed water, by using for the treatments, our no-commercial hydro-alcoholic suspensions of calcium hydroxide nanoparticles (*nanolime*). The mortars samples came from the historical site, where preliminary thermographic inspection were performed to detect the damp zones. Before treatments, the samples were analyzed from a mineralogical and chemical point of view, by means of several techniques, as optical microscopy (OM), thin section observations (PFM), porosimetric investigations, X-ray fluorescence (XRF), X-ray diffraction (XRD), infrared spectroscopy (FT-IR) and thermal analysis (TG-DTA). The size-grading curve of the aggregate and the binder/aggregate ratio were examined too. Then, the efficacy of nanolime protective treatments on this mortar versus the nanolime concentrations was investigated. For this aim, capillarity tests as well as porosimetric investigations, before and after the treatments, were performed. The obtained results were remarkably promising both in terms of the reduction of water absorbed by capillarity (up to 60 %) together with an adequate decrease of porosity (up to 23 %), fixing the protective effect of such eco-friendly and very compatible approach.
***Keywords.*** Historic mortars; Characterization; Water absorption; Protective treatments; Nanoparticles

## 1. Introduction

The knowledge and characterization of historic mortars is of great importance, in Cultural Heritage, to evaluate the conservation state of original materials, the causes of decay, and to plan an appropriate conservation work. Generally, the damaging processes affecting old lime mortars are due to chemical, physical and biological factors (*e.g.* sulphation in polluted environments, freezing-thawing cycles, and degradation by bacterial agent). Water is one of the main vehicle for such causes of decay. Actually, water damages mortar constituents, and it also dissolves salts promoting simultaneously their movement through the mortar itself; besides, water facilitates the formation of biologic colonization. These deterioration phenomena cause the loss of cohesion of the binder-aggregate system, usually followed by the superficial material loss and the reduction of mechanical strength.

The restoration of cohesion between the mortar's components is achieved by the application of organic or inorganic consolidants [1]. Generally, the intervention for restoration employs cement and polymer-based materials (*e.g.* acrylics and epoxy resins). Their use is justified by their good adhesiveness and easy methods of application, but they do not obey to the fundamental rule of physicochemical compatibility with the substrate, and they often exhibit dissimilar behaviors versus environmental conditions, causing additional damage [2, 3]. For this reason, current researches focus on the use of materials that are compatible with original substrates. At the present, lime represents the best consolidant compatible for carbonate substrates; but commercial lime, having micrometric particles [4], shows low penetration depth and incomplete carbonation process. Due to these limitations, new alternatives are recently explored as, for example, hydro-alcoholic dispersions of calcium hydroxide nano-particles (called *nanolime*), which are promising as an eco-friendly and innovative material for all carbonatic substrates or lime-based mortars. In particular, in case of historic mortars, nanolime furnishes a perfect compatibility with the original binder as well as a good penetration and high reactivity, because of their reduced particles dimensions [5-14]. In fact, once applied, during the solvent evaporation time, the nanoparticles react with atmospheric carbon dioxide and they form a thin or even nanometric calcium carbonate [8]. This calcium carbonate replaces lost binder or matrix, rebuilding the substrate, closing fine cracks and deteriorated portions of the original material. A positive

effect, resulting from that, is the increasing of strength and integrity of the mortar itself, without any unwanted residues and compounds.
The aim of the present work is to present the results of treatments based on the use of our no-commercial nanolime, carried out to protect a medieval lime mortar from absorbed water - main cause of degradation. This work, moreover, points to cover a lack of investigation about the use of nanolime on real historical mortars. The historic mortar samples come from S. Massimo D'Aveja Church, a site in a neighboring country of L'Aquila, Opi di Fagnano Alto (Italy). This Church presents a double interest, because it has been built using stones and materials coming from a Roman-Vestino temple, and it is a religious and historical site of XIV century, iconic of medieval architecture of center of Italy. The structure of the church is recently consolidated after the damage suffered during the earthquake occurred in L'Aquila (2009). In order to assess the compatibility of nanolime with the original components of the mortar, we have performed chemical and mineralogical investigations of the mortar itself. In fact, mineralogical and chemical characterization of historic mortars is fundamental both to provide useful information about the history of the monument itself, and to assist the restorers in the choice of replacement products compatible or adequate to the original ones.

## 2. Material and methods

### *2.1 Synthesis and characterization of the no-commercial nanolime*

The hydro-alcoholic nanolime suspension was synthesized in laboratory, by our patented single step procedure, as described in previous work [15-18]. In contrast to the limitations of the current nanolime syntheses [9, 18], such innovative procedure allows us to produce pure and crystalline calcium hydroxide nanoparticles in aqueous suspension, at room temperature, in few minutes and without critical separation steps, together with high yield of production. All these features are crucial when a use of nanolime is envisaged on extensive surfaces as architectural historical buildings.
For the synthesis, the following reagents were used: calcium chloride dihydrate ($CaCl_2 \cdot 2H_2O$, ≥ 99 %), supplied by Merck, anion exchange resin Dowex Monosphere 550A (OH), deionized water with a specific conductivity of 1 μS/cm (purified by a Millipore Organex System (R ≥ 18 MΩ cm)).
The pureness and phase composition of the produced nanolime suspension was characterized by X-ray powder diffraction analysis (XRD) using a *PANanlytical X'Pert* diffractometer, at $CuK_\alpha$ radiation wavelength (in the angular range from 5° to 70° 2θ). The diffraction pattern was elaborated by Profile Fit Software *HighScorePlus*, *PANalytical*, and each crystalline phase was attributed by ICSD and ICDD reference databases.
Morphology and particles dimensions were analyzed by transmission electron microscopy (TEM) and atomic force microscopy (AFM) techniques by means of *Philips CM100* microscope, and *Cypher Asylum Research* (using a cantilever Bruker model SNL10 in tapping mode), respectively. In both measurements, samples were prepared according to the standard procedures.

### *2.2 Thermography*

In order to individuate, in the building structure, the zones where the water permeates the mortar, preliminary visual and thermographic analysis of the internal and external walls of the Church [19] were carried out. In particular, the infrared inspection was performed in passive modality, in accordance with the 2012 update of the International Standard ISO 6781-1983 that outlines the general procedure for the interpretation of the infrared thermography method [20]. We used *FLIR S65 HS* thermal camera with these characteristics: detector: 320×240 pixels, spectral range: 7.5–13 μm, instant field of view: 1.1 mrad. The thermal images were processed by using Therma *CAM Reserchear Pro 2.10* software, supplied by FLIR.

### *2.3 Mineralogical and chemical characterization of the historic mortar*

The mortar analysis was carried out on the whole samples (the binder plus the aggregate) and then on the binder and on the aggregate, separately. In particular, all the investigations on whole mortar samples were performed before and after the nanolime treatments, repeated for three times.
A general examination of structure and texture of the mortar has been performed using a stereomicroscope, (SM, *Leica Stereozoom S8 APO*), and specific investigations were carried on by observations of thin-sections, using polarization-fluorescence microscopy (PFM, *AXIO Scope A1-Zeiss*).
In the decay processes, pores play a major role driving the diffusion of the water inside the mortars; at the same time, they are the sites where most of the physical-chemical processes associated to weathering and

biological phenomena occurs and where the treatments act into the sample. For this reason, porosity was measured by means of combined instruments, using both *AccuPyc 1330-Micromeritics* pycnometer and *GeoPyc 1360-Micromeritics* density analyzer. Twenty fragments of mortar of about 1 cm in dimension were analyzed and a statistical analysis was also performed, reporting the mean value and the standard deviation as statistical error.
In this study, the binder was separated from the aggregates in order to obtain knowledge on single components, aggregate size distribution, binder/aggregate ratio [20], and to characterize the aggregates from a petrographic point-of-view, by means of a visual analysis [21]. 350 g of mortar samples were gently crushed and dried in oven at 60°C until mass constancy was reached. After this, the aggregate size distribution was obtained by sieving the sample through a standard series, attributing the fine fraction passing the 63 μm sieve to the binder-enriched fraction, and the retained one to the aggregate fraction as well [22, 23].
The binder and the aggregate fractions were characterized by means of several techniques, as X-Ray Fluorescence spectrometry - XRF (*X Spectro-Xepos III*), XRD (*PANanlytical X'Pert* diffractometer), as well as infrared spectroscopy - FTIR (*Thermo Nicolet spectrophotometer Nexus*). In particular, XRD patterns were recorded in the angular range from 5° to 70° 2θ, (steps size of 0,026° 2θ; time per step 400 sec). Each experimental diffraction pattern was elaborated by the Profile Fit Software, and crystalline phases were attributed by ICSD and ICDD reference databases. A quantitative estimation of the phase percent was obtained by means of the Reference Intensity Ratio (RIR) method [24]. FTIR analyses were recorded in the 4000-400 $cm^{-1}$ region at a resolution of 4 $cm^{-1}$. Thermal analyses were performed with a *LINSEIS L.81* thermobalance, thermal analyzer system, in a controlled heating from ambient temperature up to 1000 °C in a static air atmosphere, with a temperature gradient of 10 °C$min^{-1}$.

*2.3 Nanolimes treatments and analysis of their effectiveness*

Our nanolime can be tailored for any specific treatment, changing in an easy way both solvent and concentration. In this case, two suspensions at two different concentrations were prepared: 25 g/l and 50 g/l, considering for both 10 % water volume with 90 % of ethanol. Ethanol enhances the dispersion stability and penetration ability of the nanolime particles inside the treated materials [25]. Three specimens of the original mortar were chosen, for each nanolime concentration, named S$i_{25}$ and S$i_{50}$ (i=1, 2, 3). They were partially immersed for 30 minutes in the nanolime suspensions, according to procedure reported in literature [3, 7, 26, 27], and then, in order to enhance the nanolime carbonation process, they were put in a chamber at controlled relative humidity (R.H. 90 %) for 24 hours. After, the specimens were dried in a oven at 60°C up to a constant mass value. This protocol was defined to obtain very reproducible laboratory treatments and it was applied either one or three times.
The efficacy of nanolime treatment was determined measuring the water adsorbed by capillarity before and after treatment, by means of the procedure in [28]. The mortar specimens were brushed to remove free particles, weighed, and the most flat face was put in contact with water on a wet gauze, not directly immersed in water. Each sample was weighed at 10, 20, 30 minutes, 1, 2, 3, 24, 48 and 72 hours and the amount of absorbed water by the specimen per unit area $Q_i$ (kg/$m_2$), at time $t_i$ (s), is calculated as in Eq. (1):

$$Q_i = \frac{[(m_i - m_0)]}{A} \qquad (1)$$

where, $m_i$ is the weight at each time interval, $m_0$ is the initial weight, and $A$ is the sample surface area. The resulting $Q_i$ were reported versus square root of time ($t_i^{1/2}$). In this representation, the capillary water absorption (AC) were the slope of the curve. The effective protective efficacy $E_p$ was defined as the percentage variation of $Q_i$ value before and after treatment.

## 3. Results and Discussion

*3.1. Characterization of the mortar*

Representative mortar samples are chosen from the wall of the facade, corresponding to the apse and to the lateral front, presenting the highest decay due to the absorption of capillary water. In particular, from thermography (*Fig. 1*) it can be distinguished two damaged areas; the damp area on the East wall can be attributed to moisture percolation, while the one individuated on the North wall was related to the rising damp effect from the soil.

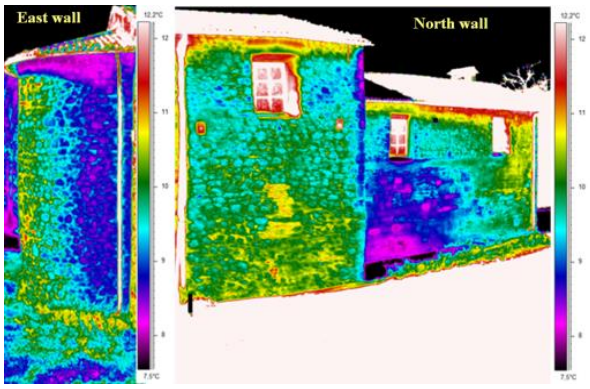


**Figure 1.** Thermogram of the North and East walls of the Church

The mortar specimen, observed by stereomicroscope, is a heterolithic aggregate of carbonaceous (limestone) clasts, with an open-framework structure, being the clasts sustained by a microcrystalline matrix. Between the clasts are present open spaces, irregular vugs, more abundant in the central part of the sample. The carbonaceous clasts can be divided into two different granulometric size groups, one with diameter ranging from 3 to 6 mm, the other with diameter < 1 mm. In particular, the binder seemed to be uniformly dispersed, and sample presents irregular and jagged sides (*Fig. 2*).

***a)*** 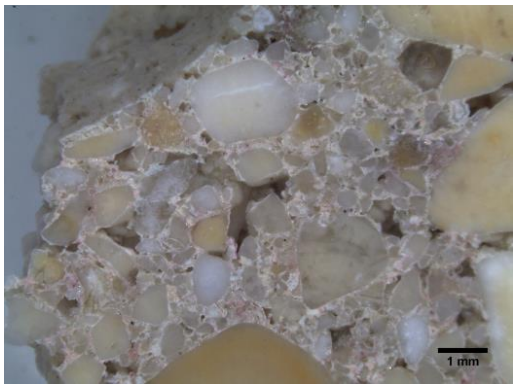

***b)*** 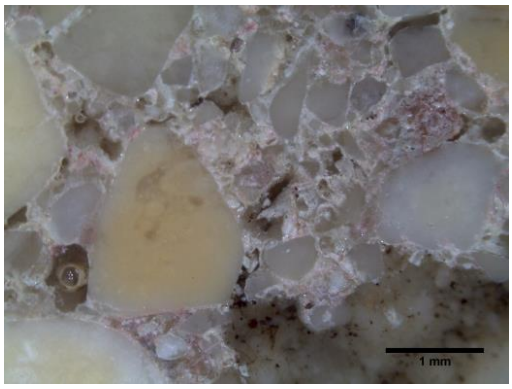


**Figure 2.** Optical images of the untreated mortar specimen, acquired at different magnifications.

From the thin section observation, reported in *Fig. 3*, the larger limestone clasts are rounded to sub-rounded and some are broken; they are classified on a geo-lithological base as mudstone, packstone, wackestone and oolitic-bioclastic grainstone. The smaller limestone clasts are instead mainly sub-angular and can be classified as mudstones. To be noted that the matrix surrounds almost all the clasts, but still some empty vugs are present (*Fig. 3b)*). Considering the grade of roundness of the two clasts type, it can be assessed that they have been collected from two different deposits: the larger are from a riverbed or alluvional type deposit, the smallest one instead are from a mountain debris talus. In the larger clasts can be found gastropods (*Fig. 3c)*, benthonic biseriate micro-foraminifera *nummulitidae* types, algae fragments like *dasidaclaceae* and *solenoporacee*. The clasts are hold together by dense crypto crystalline matrix not resolved with optical microscope (*Figg. 3b-c)*). As a whole, considering their classification and fossil content, it can be assessed that the limestone rock types, (forming the granular structure of the sample), were formed in a carbonatic platform environment. The micro paleontological species recognised suggest that the carbonaceous clasts derive from the erosion of limestones having an age comprises between Cretaceous Sup. and Miocene. The limestones, having age and geolithological characteristics suitable with the clasts in the sample, crop out in the area of Monte D'Ocre (L'Aquila-Italy).

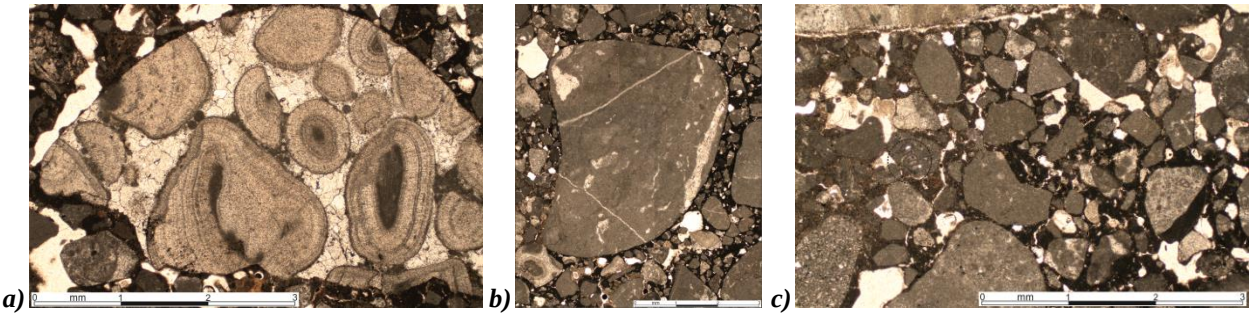

**Figure 3**. Optical microscope images (2.5x magnification). ***a)*** oolitic grainstone clast. The limestone clast is broken; ***b)*** The larger clast in the centre is a wackestone and is well rounded. The smaller clasts around it have instead sub-angular outlines; ***c)*** Detail of the clasts having diameter < 1 mm that are suspended in the dark and dense matrix. The black circle indicate the gastropod fossil.

Subsequently, the binder and the aggregate, after the mechanical separation and sieving procedure, were analysed. The size-grading curve of the aggregate, corresponding to the percentage weight respect to each sieved fraction, was obtained: 19.5±0.5 % of mortar is binding material (< 63 μm) and 80,5±0.5 % is the aggregate fraction (grain size between 63 and 1400 μm). This evaluation allows estimating the binder/aggregate ratio equal to 1:4 which corresponds to that referred to same historical period of the S. Massimo Church [29, 30]. According to the standard procedure, by a visual observation of the coarser fraction of the mortar aggregate, individual clasts appear constituted by: a) 42 % of coarse sub-angular to sub-rounded grains, poor selected; b) 14 % of fine sub-rounded aggregates; c) 44 % of arenaceous ones.
The elemental composition of both the binder and aggregate fractions, obtained by XRF, is reported in Table 1.

**Table 1.** XRF analysis on the mortar constituents (wt %).

| | **Ca** | **Si** | **Al** | **Fe** | **Mg** | **K** | **Cl** | **S** | **Na** | **P** |
|---|---|---|---|---|---|---|---|---|---|---|
| *Binder (<63 μm)* | 33.99 | 3.81 | - | 0.71 | 0.61 | 0.23 | 0.16 | 0.12 | - | 0.11 |
| *Aggregate* | 23.09 | 2.55 | 0.89 | 0.42 | 0.25 | 0.35 | - | 0.11 | 0.17 | 0.10 |

The mineralogical analysis of the aggregate shows that it is composed by 97% of calcite ($CaCO_3$, ICSD pattern 98-002-8827), 2% of quartz ($SiO_2$, ICSD pattern 98-006-2406) and traces of muscovite ($Al_3Si_3K(OH)_2O_{10}$, ICSD pattern 98-000-9650) (*Fig. 4a)*). The binder is composed by 93% of magnesium calcite crystalline phase ($C_1Ca_{0.94}Mg_{0.06}O_3$, ICSD pattern 98-008-6162) and by 7% of quartz ($SiO_2$, ICSD pattern 98-006-2406) deriving from the contamination with very thin particles passed from the sieving process (*Fig. 4b)*), and confirmed by XRF analysis.

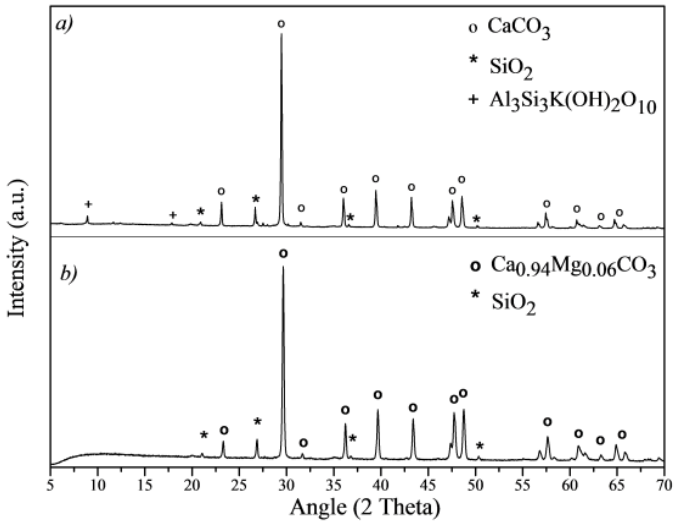


**Figure 4.** XRD patterns of the mortar samples; ***a)*** aggregate fraction; ***b)*** binder fraction.

These results are confirmed by the FT-IR analyses, for both fractions, which mainly present all the typical absorption bands of calcite at 2515, 1799, 1423, 875 and 713 $cm^{-1}$. The presence of free water (band at 3400 $cm^{-1}$, and at 1630 $cm^{-1}$) and of Si-O vibration at around 1040 and 470 $cm^{-1}$ [30] is observed too.
As concerns TG-DTA measurements, both the binder and the aggregate fraction have an endothermic peak at around 100 °C, which can be attributed to physically adsorbed water. In addition, a weight loss less than 1% is observed during the heating up phase, up to 100 °C, revealing that mortar do not show a hygroscopic behavior [20]. It has been also observed a strong endothermic peak at about 860 °C for the binder and 900 °C for the coarse fraction, in relation to a weight loss of about 36% and 41% respectively, attributable to calcite decomposition, as detected by the XRD analyses. The shift in temperature for this endothermic peak, observed for the binder, can be attributed to the presence of magnesium in the calcite lattice [31], but also to different crystal sizes of calcite in the binder particles compared to that of the aggregate sample.

*3.2. Characterization of the nanolime suspension used in the treatments*

From XRD analysis (*Fig. 5*), the nanolime suspension, used for the treatments, is composed by pure and crystalline phase of hexagonal Portlandite (ICSD#96-100-8782, $Ca(OH)_2$).

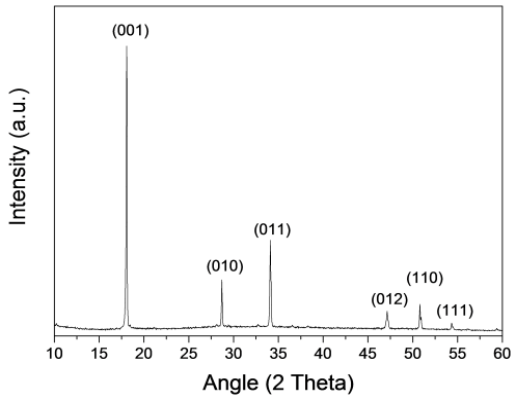


**Figure 5.** XRD pattern of dried particles from the synthesized nanolime suspension. Bragg peaks of $Ca(OH)_2$ pattern (ICSD#96-100-8782) are indexed.

The nanolime particles, as determined by TEM observations, present a hexagonal morphology, formed by the aggregation of $Ca(OH)_2$ nanocrystals with small dimensions, finely dispersed (*Fig. 6a)*). These results are supported by AFM analysis (*Fig.6b)*) which shows a single nanoparticle less than 50 nm in diameter and 5 nm in height (Z-direction).

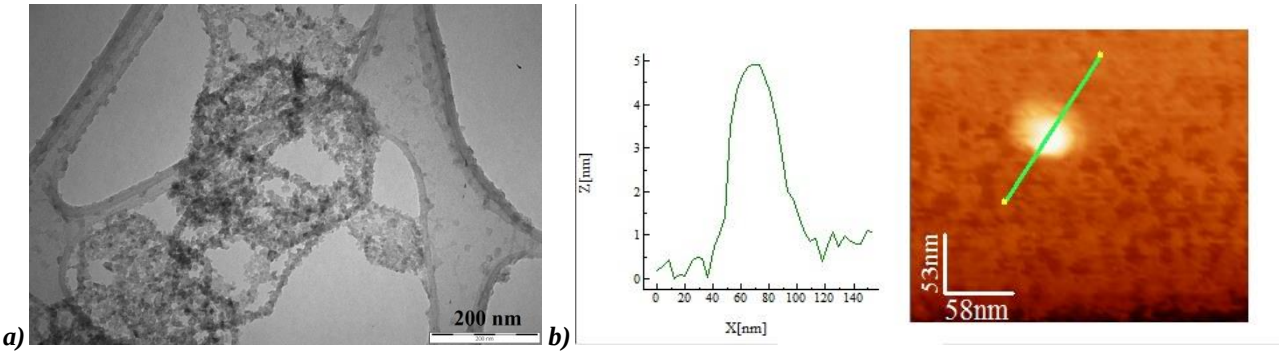


**Figure 6.** Microscopic observations of the synthesized nanoparticles: ***a)*** TEM image referred to the $Ca(OH)_2$ nanocrystals; ***b)*** AFM image of a single particle (right), and the profile analysis along the Z-axis (left).

*3.3. Efficacy of nanolime treatments*

Optical image of a sample treated with nanolime suspension at concentration of 25 g/l, is reported in *Fig. 7a)*. It is possible to note that the treated surface appears less wrinkled and further homogeneous, with reduced superficial discontinuities if compared to the untreated sample (*Fig.2a)*). It can be also observed a "white layer" on the surface, related to the nanolime treatment. The sample treated with a concentration of 50

g/l, reported in *Fig. 7b)*, is characterized by the said layer on the surface without diffusion of lime into the superficial cavities, as instead observed at lower concentration (25 g/l).

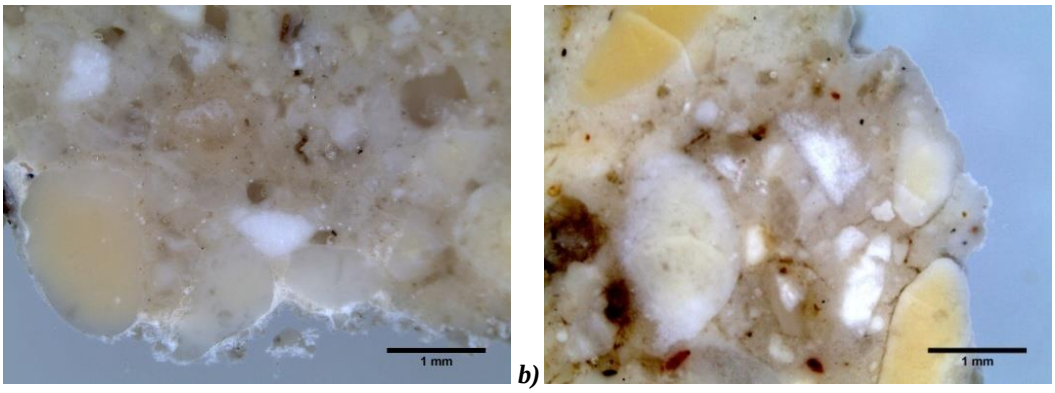


**Figure 7.** Mortar samples treated with nanolime suspensions at different concentrations. ***a)*** 25g/l; ***b)*** 50g/l.

Thin section observations, reported in *Fig.8*, show in the treated area two different types of matrix, holding the clasts. In particular, since the treatment has been done by immersion, the nanolime penetration in the sample is from outside to inside. From the external part of the sample inwards, a variation in the matrix color, accompanied by a change in the microstructure, can be distinguished. The external portion is paler, cream in color and there are birifrangent crypto-crystals emerging from the dense and opaque matrix. The darker internal part, instead, do not contain crypto-crystals. In the treated portion of the sample, although some irregular vugs are still present, all the clasts are well coated by the creamish binder. The depth of the treatment infiltration is variable between 2 and 2.5 mm, and it results homogeneous in the treated volume.

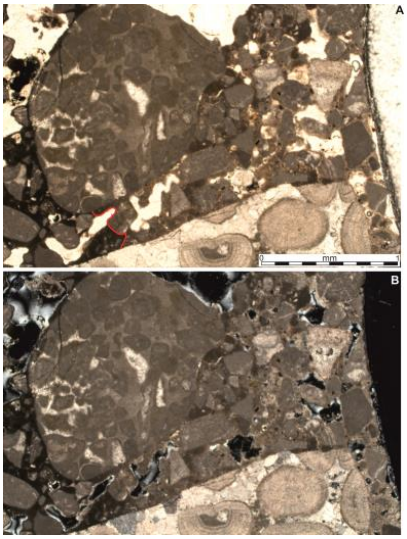


**Figure 8.** Optical microscope image (5x magnification). Top image: (light with normal polarization), transition between the external creamish colored matrix and the darker internal matrix (outlined by the red line) is shown. Down image: (cross polarized light), the external matrix shows the presence of birifrangent crypto-crystals.

These observations are consistent with the results of porosimetric investigation, where it can be observed a reduction of the superficial porosity from (31±6)%, before treatment, to (26±8)% and (15±4)% after treatments at suspension concentrations of 25 g/l and 50 g/l, respectively. Moreover, from these results the nanolime treatment seems to reduce the superficial porosity, as much as the concentration of suspension increases.

The nanolime treatment effectiveness also towards water was evaluated by measuring the reduction of water absorbed by capillarity, in the treated samples compared to the untreated ones. These results are very significant, in particular when the mortar is repetitively exposed to freeze-thawing cycles, as it is the case in Abruzzo region where the S. Massimo D'Aveja Church is located, as well as in all historical building placed in cold regions. In *Fig.9* are reported the results of water absorbed by capillarity from the mortar samples before and after treatments, including the capillary water absorption coefficient (AC).

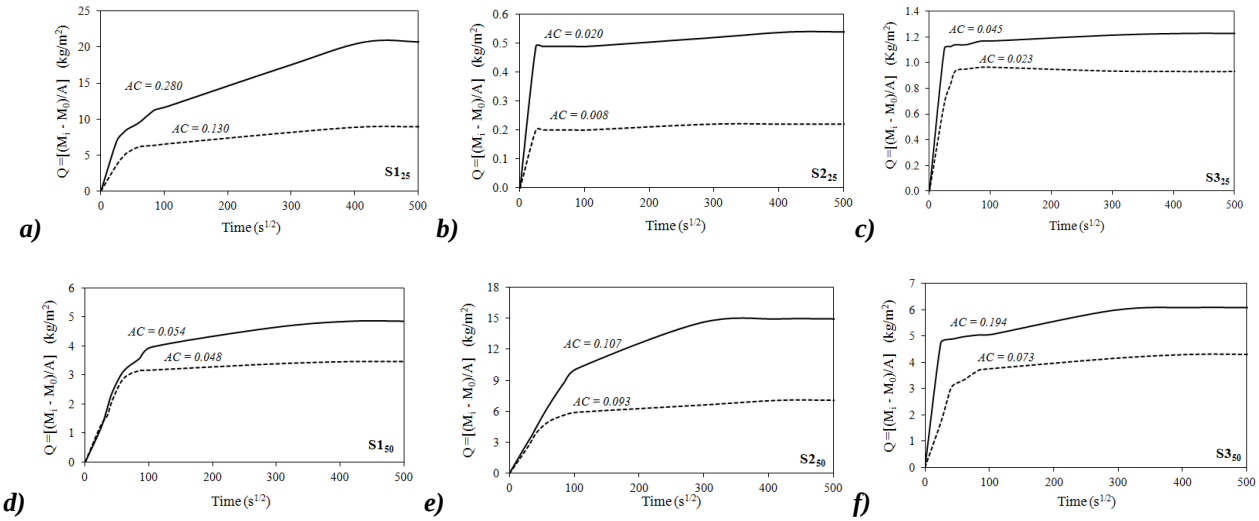


**Figure 9.** Capillarity curves of mortar samples before (continuous lines) and after (dot lines) three repeated treatments: ***a-b-c)*** at a nanolime concentration of 25g/l; ***d-e-f)*** at a nanolime concentration of 50g/l. AC values are reported too.

Taking into account that the AC coefficient can be directly related to the pore sizes, the results coming from the capillarity tests match with previous ones from optical microscopy and porosity measurements. In fact, a percentage reduction of AC coefficient up to 70% results, corresponding to a formation of a thin coating of stable calcium carbonate on the surface of the superficial pores, which reduces their diameter. Moreover, the treatments performed at 25g/l determine an AC reduction for all the treated samples, while in the case of higher nanolime concentration only one sample presents an AC reduction (*Fig. 9f*). The total water amount absorbed by capillarity appears, instead, clearly reduced in all treated samples. The results of protective efficacy $E_p$, in fact, underline a high protective effect of the nanolime treatments, already after only one protocol, for both concentration values. In particular, the treatment performed with a nanolime concentration of 25 g/l shows the best $E_p$ value ranging from 16 % to 40 %, after only one protocol. According to the protocol, after three treatments, the $E_p$ values continue to increase, up to about 60 % for two of the three considered samples. Treatments performed at a 50 g/l nanolime concentration, reveal lesser $E_p$ values, together with a less reduction of the AC index. The last result can be ascribed to the higher agglomeration of nanoparticles that limits their penetration towards the internal pores of the material, as observed from the stereomicroscope optical images. At the same time, the agglomerated particles cover the surface reducing the pores, leading to the formation of a thicker calcium carbonate coating as well, which can be less adherent to the substrate and, consequently, it is less protective in presence of water.
Finally, it is important to underline that the porosity reduction, here observed, is an important perspective not only towards the water protection but also because it can positively influence the superficial mechanical properties of the mortar itself, as also reported in literature [1, 3, 32].

## Conclusions

In this work, representative medieval mortar samples from damaged areas of the San Massimo d'Aveja Church were collected and characterized from mineralogical and chemical point of view. In particular, the collected samples resulted constituted by a magnesium lime binder and an aggregate mainly composed by calcium carbonate, coming from the erosion of local limestones having an age between Cretaceous Sup. and Miocene. Moreover, the mortar are characterized by a binder/aggregate ratio of 1:4; the aggregate distribution in the binder seemed to be well homogeneous, and mainly constituted by fine to coarse sub-angular and sub-rounded clasts. The lime mortar was characterized by a binder matrix constituted by pores of variable size and by an irregular and jagged side, giving a medium porosity of about 31 %. In order to evaluate protection efficacy towards water absorbed by capillarity, treatments have been carried out using no-commercial hydro-alcoholic nanolime suspensions, employed at different concentrations. Nanolime was synthesized by our innovative, time and energy-saving route based on an exchange ion process. From optical images, the surfaces of the treated mortar samples appeared less wrinkled and further homogeneous respect to the untreated ones. A porosity reduction up to 15 % was observed too. For all treated samples, the saturation water value absorbed by capillarity was clearly reduced, with a protective efficacy up to about 60 %, for both the suspension concentrations. Moreover, the nanolime treatment, performed at low

concentration, covered the superficial pores, penetrating up to 2,5 mm from the surface, filling the surface of the pores by a crypto-crystalline coating of stable calcium carbonate.
In conclusion, our nanolime can represent an excellent material for the restoration and preservation of the historic mortars in an efficient (and economic) way. In particular, it combines this efficacy with a perfect physico-chemical compatibility with the original historic lime mortar.

**Acknowledgments.** The authors gratefully acknowledge to Ms. Tonina Rosa, Chairwoman of the Opi Onlus Association (L'Aquila, Italy), for her valuable willingness. The experimental assistance on TEM and optcal observations of Dr. Lorenzo Arrizza and Dr. Maria Giammatteo, Center of Microscopy (University of L'Aquila), is gratefully acknowledged. Thanks also to Ms. Fabiola Ferrante, Department of Industrial and Information Engineering and Economics (University of L'Aquila), for her kind collaboration.

**References**

[1] Borsoi, G. et al. (2012) Microstructural and physical-mechanical analyses of the performance of nanostructured and other compatible consolidation products for historical renders. *Materials and technology* 46, 223–226. UDK 691:620.1:691.5, ISSN 1580-2949.
[2] Maravelaki-Kalaitzaki, P. et al. (2015) Hydraulic lime mortars for the restoration of historic masonry in Crete. *Cement and Concrete Research* 35, 1577-1586. DOI:10.1016/j.cemconres.2004.09.001.
[3] Daehne, A.; Herm, C. (2013) Calcium hydroxide nanosols for the consolidation of porous building materials, *EU-STONECORE*, Daehne and Herm Heritage Science, 1-11.
[4] Mascolo G.; Mascolo M.C.; Vitale A.; Marino O. (2010) Microstructure evolution of lime putty upon aging, *Journal of Crystal Growth* 312, Issues 16-17, 1-15, 2363-2368. DOI: org/10.1016/j.jcrysgro.2010.05.020.
[5] Baglioni, P.; Giorgi, R. (2006) Soft and hard nanomaterials for restoration and conservation of cultural heritage, *Soft Matter* 2, 293-303. DOI: 10.1039/B516442G.
[6] Ziegenbalg, G.; Brümmer, K.; Pianski, J. (2010) Nano-lime - a new material for the consolidation and conservation of historic mortars, 2nd Conference on Historic Mortars - HMC 2010 and RILEM TC 203-RHM final workshop, e-ISBN: 978-2-35158-112-4, Publisher: RILEM Publications SARL, 1301-1309.
[7] D'Armada, P.; Hirst, E. (2012) Nano-Lime for Consolidation of Plaster and Stone, *Journal of architectural conservation* 18, 63-80. DOI: 10.1080/13556207.2012.10785104.
[8] Daniele, V.; Taglieri, G. (2012) Synthesis of a nanolime by using Triton X-100 and protective treatments on natural stones: preliminary results, *Journal of Cultural Heritage* 13, 40-46. DOI: 10.1016/j.culher.2011.05.007.
[9] Rodriguez-Navarro, C.; et al. (2013) Alcohol dispersions of calcium hydroxide nanoparticles for stone conservation, *Langmuir* 29 [36], 11457-70. DOI: 10.1021/la4017728.
[10] Drdácký, M.; Slížková, Z.; Ziegenbalg, G. (2009) A Nano Approach to Consolidation of degraded Historic Lime Mortars. *Journal of Nano Research* 8, 13-22. DOI:10.4028/www.scientific.net/JNanoR.8.13.
[11] Middendorf, B.; et al. (2005) Investigative methods for the characterisation of historic mortars-Part 1: Mineralogical characterisation, *Materials and Structures* 38, 761-769. DOI:10.1617/14282.
[12] Daniele, V.; Taglieri, G.; Quaresima, R. (2008) The nanolimes in Cultural Heritage Conservation: characterisation and analysis of the carbonatation process, *J. Cultural Heritage* 9, 294-301. DOI: 10.1016/j.culher.2007.10.007.
[13] Daniele, V.; Taglieri, G. (2011) $Ca(OH)_2$ nanoparticles characterization. Microscopic investigation of their application on natural stones, In: *"Materials Characterisation V - Computational Methods and Experiments",* A.A. Mammoli, C.A. Brebbia, A. Klemm, Wit press, Southampton, UK, pp.55-66. ISBN: 978-1-84564-538-0. Published also in: WIT Transaction on Engineering Sciences, Vol.72, ISSN:1746-4471 (print), 1743-3533 (on-line).
[14] van Hees, R.P.J.; et al. (2014) Compatibility and performance criteria for nano-lime consolidants, In: *Proceedings of the 9th International Symposium on the Conservation of Monuments in the Mediterranean Basin*, Ankara, 3-5 June (2014).
[15] Volpe, R.; Taglieri, G.; Daniele, V.; et al. (2012) A process for the synthesis of $Ca(OH)_2$ nanoparticles by means of ionic exchange resin. Priority RM2011A000370, WO2014020515A1 (2012).
[16] Taglieri, G.; Felice, B.; Daniele, V.; Volpe, R.; Mondelli, C. (2016) Analysis of the carbonatation process of nanosized $Ca(OH)_2$ particles synthesized by exchange ion process, *Proceedings of the Institution*

*of Mechanical Engineers, Part N: Journal of Nanoengineering and Nanosystems* 230, Issue 1, 25-31. DOI: 10.1177/1740349914537616.
[17] Taglieri, G.; Daniele, V.; Del Re, G.; Volpe, R. (2015) A new and original method to produce $Ca(OH)_2$ nanoparticles by using an anion exchange resin, *Advances in Nanoparticles* 4, 17-24. DOI: 10.4236/anp.2015.42003.
[18] Aniruddha, S.; Dipak, K.C. et al. (2015) Synthesis of Nano Calcium Hydroxide in Aqueous Medium, *J. Am. Ceram. Soc.*, 1–9. DOI: 10.1111/jace.14023.
[19] Sfarra, S.; Marcucci, E.; Ambrosini, D.; Paoletti, D. (2016) Infrared exploration of the architectural heritage: from passive infrared thermography to hybrid infrared thermography (HIRT) approach, *Materiales de Construcción* 66, Issue 323, e094, 1-16.
[20] Maravelaki-Kalaitzaki, P.; et al. (2003) Physico-chemical study of Cretan ancient mortars, *Cement and Concrete Research* 33, 651–661. DOI: 10.1016/S0008-8846(02)01030-X.
[21] UNI 11176 (2006) Cultural heritage. Petrographic description of a mortar.
[22] UNI 11305 (2009), Cultural heritage. Historical mortars. Guideline for the mineralogical-petrographycal, physical and chemical characterization of mortars.
[23] Moropoulou, A.; Bakolas, A.; Bisbikou, K. (2000) Investigation of the technology of historic mortars, *Journal of Cultural Heritage* 1, 45-58. DOI: 10.1016/S1296-2074(99)00118-1.
[24] Bish, D.L.; Post, J.E. (1989) Modern Powder Diffraction, *Reviews in Mineralogy* 20, ISSN 0275-0279; ISBN 0-939950-24-3.
[25] Daniele, V.; Taglieri, G. (2010) *Nanolime* suspensions applied on natural lithotypes: the influence of concentration and residual water content on carbonatation process and on treatment effectiveness, *Journal of Cultural Heritage* 11, 102–106. DOI: 10.1016/j.culher.2009.04.001.
[26] Moreau, C.; Slížková, Z.; Frankeová, D.; Drdácký, M. (2010) Effects of impregnation of mortars with nano-lime on their physical characteristics, in: *Recent progress in the consolidation of calcareous materials - STONECORE*, Litomyšl, Czech Republic, 21/22 April 2010, 18.
[27] Arizzi, A.; Gomez-Villalba, L.S.; Lopez-Arce, P.; Cultrone, G.; Fort, R. (2015) Lime mortar consolidation with nanostructured calcium hydroxide dispersions: the efficacy of different consolidating products for heritage conservation, Eur. J. Mineral. PrePub. DOI: 10.1127/ejm/2015/0027-2437.
[28] Veiga, M.R.; Magalhães, A.C.; Bokan-Bosilikov, V. (2004) Capillarity tests on historic mortar samples extracted from site. Methodology and compared results, *13th International Brick and Block Masonry Conference*, Amsterdam (2004).
[29] Riccardi, M.P.; et al. (1998) Thermal, microscopic and X-ray diffraction studies on some ancient mortars, *Thermochimica Acta* 321, 207-214.
[30] Silva, D.A.; Wenk, H.R.; Monteiro, P.J.M. (2005) Comparative investigation of mortars from Roman Colosseum and cistern, *Thermochimica Acta* 438, 35-40. DOI:10.1016/j.tca.2005.03.003.
[31] M. Rao Dasari (1986), Lattice variations in natural magnesium calcites, *Thermochimica Acta* 101, 385-387.
[32] Slížková, Z.; Frankeová, D. (2012) Consolidation of porous limestone with nanolime. Laboratory study, *12th International Congress on the Deterioration and Conservation of Stone*, Columbia University, New York, 2012.